Journal of the Serbian Chemical Society

JSCS-info@shd.org.rs • www.shd.org.rs/JSCS

J. Serb. Chem. Soc. 75 (7) 965–973 (2010)
JSCS–4022

UDC 666.32+661.182+66.094.3:61.000.57
Original scientific paper

Singlet oxygen generation by higher fullerene-based colloids

SVETLANA P. JOVANOVIĆ[1]*, ZORAN M. MARKOVIĆ[1], DUŠKA N. KLEUT[1], VLADIMIR D. TRAJKOVIĆ[2], BRANKA S. BABIĆ-STOJIĆ[1], MIROSLAV D. DRAMIĆANIN[1] and BILJANA M. TODOROVIĆ MARKOVIĆ[1]

[1]*Vinča Institute, P.O. Box 522, 11001 Belgrade and* [2]*Institute of Microbiology and Immunology, School of Medicine, University of Belgrade, Dr. Subotića 1, 11000 Belgrade, Serbia*

(Received 17 June 2009, revised 26 April 2010)

Abstract: In this paper, the results of the synthesis and characterization of higher fullerene-based colloids is presented. The generation of singlet oxygen ^{1}O2 ($^1\Delta$g) by fullerene water-based colloids (*n*C60, *n*C70 and *n*C84) was investigated. It was found by electron paramagnetic resonance spectroscopy that the generation of singlet oxygen was the highest by the *n*C84 colloid. The amplitude of the electron paramagnetic resonance (EPR) signal was two orders of magnitude higher than the amplitude of the EPR signals which originated from *n*C60 and *n*C70. The surface morphology and the structure of the particles of the water-based colloids were investigated by atomic force microscopy (AFM). The AFM study showed that the average size of the *n*C60, *n*C70 and *n*C84 were 200, 80 and 70 nm, respectively. In addition, the particle size distribution of the *n*C60, *n*C70 and *n*C84 colloids was determined by dynamic light scattering (DLS) measurements.

Keywords: higher fullerene; colloid; electron paramagnetic resonance spectroscopy; atomic force microscopy; dynamic light scattering.

INTRODUCTION

For more than 20 years, fullerenes have attracted the attention of researchers from many different fields. Their application is possible in many areas (biomedicine, electronics) because of their unique properties.[1–6] Whereby, their photophysical properties are the most interesting for medical applications. Pristine fullerenes, C_{60} [60-I_h] and C_{70} [70-D_{5h}], effectively produce singlet oxygen ($^1\Delta_g$) by absorbing light energy.[7] The photosensitized production of singlet oxygen involves four steps: a) absorption of light; b) formation of the triplet state of the photosensitizer; c) trapping of the triplet state by molecular oxygen; d) energy transfer from the triplet state to molecular oxygen.[8] In photodynamic therapy

* Corresponding author. E-mail: svetlanajovanovic@vinca.rs
doi: 10.2298/JSC090617062J

(PDT) of cancer, fullerenes could be used as photosensitizers.[9] Photodynamic therapy (PDT) is one of the non-invasive treatments applicable with reduced side effects for various types of tumors.[10] Chemical modification by PEG of appropriate molecular weight and terminal structures enables water-insoluble C_{60} to dissolve in water and automatically accumulate in a tumor. The PDT effect of C_{60}-PEG-Gd was significant when light irradiation was performed 3 h or longer after injection, whereas no effect was observed 1 h after injection.[11]

Biomedical applications demand fullerene in a water soluble form. Several methods have been developed to disperse these otherwise hydrophobic carbon compounds in water.[12] There are different methods for creating colloidal nanocrystalline fullerenes ($n$$C_{60}$, $n$$C_{70}$ and $n$$C_{84}$).[13–15] Variations such as the solvent used, temperature, fullerene concentration and mixing regime affect the size, structure and charge characteristics of fullerene-based colloids. Differences in size, structure and surface chemistry of $n$$C_{60}$ produced by various procedures could have important implications for the interpretation of data from environmental transport and toxicity studies.

In a previous study, it was shown that $n$$C_{60}$ intercalated with different solvents produce singlet oxygen at different rates.[16] With regard to their capacity to generate ROS and cause mitochondrial depolarization followed by necrotic cell death, $n$$C_{60}$ suspensions are ranked in the following order: THF/$n$$C_{60}$ > EtOH/ /$n$$C_{60}$ > aqua/$n$$C_{60}$. Mathematical modeling of singlet oxygen ($^1\Delta_g$) generation indicates that the $^1\Delta_g$-quenching power (THF/$n$$C_{60}$ < EtOH/$n$$C_{60}$ < aqua/$n$$C_{60}$) of the solvent intercalated in the fullerene crystals determines their ability to produce ROS and cause cell damage.

In this study, singlet oxygen generation of fullerene-based colloids was investigated. The photophysical properties of higher fullerenes remain poorly understood, largely because of the challenge posed by multiple isomeric forms of these compounds.[17] Singlet oxygen was detected by electron paramagnetic resonance (EPR) spectroscopy, following the formation of stable nitroxide radicals, TEMPO (2,2,6,6-tetramethylpiperidine-1-oxyl).[18] Using atomic force microscope (AFM), individual particles and group of particles can be visualized and unlike other microscopy techniques, AFM offers visualization in three dimensions. Based on dynamic light scattering (DLS) analysis, it was found that the average size of the higher fullerene colloidal particles was about 40 nm.

EXPERIMENTAL

C60 (99.9 % purity), C70 (99 % purity) and mixture of higher fullerenes (C84 (40 %), C76 (20 %), C78 (20 %) and C70 (20 %) - further in the text C84) were purchased from MER corporation, Tuscon, USA. The preparation procedure of nC60 and nC70 were described in previous studies.[16,19] Freshly distilled THF of HPLC purity (Carlo Elba, Milan, Italy) was used as the solvent. During the preparation of nC84/THF, powder of the higher fullerenes was added to THF at a concentration of 10 mg L^{-1}. The THF/C84 mixture was purged with nit-

rogen to remove any dissolved oxygen and stored overnight in the dark while being continuously stirred to ensure a homogeneous mixture. The THF/C84 solution was then filtered through a 0.5 μm PTFE filter to remove any excess of solid material. An equal amount of MilliQ water was then added to the THF/C84 filtrate at a rate of 1 L min^{-1} under continuous stirring. The THF was removed from the solution using a rotary evaporator operated at 45 °C. The concentrations of fullerene particles in water were determined from the absorption spectra. The concentration of the THF/*n*C84 suspension was approximately 6 mg L^{-1}.

Silicon was used as the substrate. The drop of fullerene-based colloids was deposited on silicon substrates and dried in air. The morphology of the three different colloids was investigated by means of a Quesant AFM. A conventional Si cantilever was used for all measurements under ambient conditions. Imaging was realized in the non-contact dynamic mode. In this mode, the cantilever oscillates close to resonance and the tip only slightly touches the surfaces. All images were processed for better quality.

The particle size distributions of the C^{60}, C^{70} and higher fullerene suspensions were obtained using a Brookhaven Instruments light scattering system equipped with a BI-200SM goniometer, a BI-9000AT correlator, a temperature controller and a Coherent INNOVA70C argon-ion laser.

EPR Spectroscopy was used to monitor the generation of singlet oxygen in the aqueous solutions. The EPR experiments were performed at room temperature using a Varian E-line spectrometer operating at a nominal frequency of 9.5 GHz. A mixture containing 0.18 mL TMP (Sigma) and different fullerene-based colloids with a concentration of 2 mg L^{-1} was thoroughly ultrasonicated and incubated at room temperature for 24 h. Aliquots (7 μL) of the TMP-fullerene mixtures were then transferred into 3 mm i.d. quartz tubes and the Tempol signal was analyzed by EPR. Quantification of the signals was realized by calculating the mean value of the amplitudes of the EPR signals and the data are expressed in arbitrary units.

RESULTS AND DISCUSSION

Surface morphology

In addition to yielding three-dimensional topographic images of investigated objects, AFM has also become an invaluable tool for studying important properties of a specimen.[20] The surface morphology of the prepared fullerene-based colloids deposited on freshly cleaned silicon substrates was observed by atomic force microscopy. The size and shape of particles of the three different fullerene-based colloids were determined by AFM. The colloids were diluted to a concentration of approximately 0.1 mg L^{-1} to prevent agglomeration of particles during the course of drying and to enable the detection of single particles. The AFM images of the particles of the nC_{60}, nC_{70} and nC_{84} colloids are presented in Figs. 1a–1f. As can be observed from Fig. 1, the average sizes of the nC_{60}, nC_{70} and nC_{84} particles based on surface profile analysis were 200 nm, 80nm and 70 nm, respectively.

Despite the precautions, the particles formed agglomerates on certain areas of the silicon substrate. It is considered that most of the aggregates were formed during drying but preformed aggregates, maintained by van der Waals attraction, in the colloid are also possible.[21] Brant *et al*. observed that aggregate formation resembled a crystal growth process rather than undirected particle aggregation.[22]

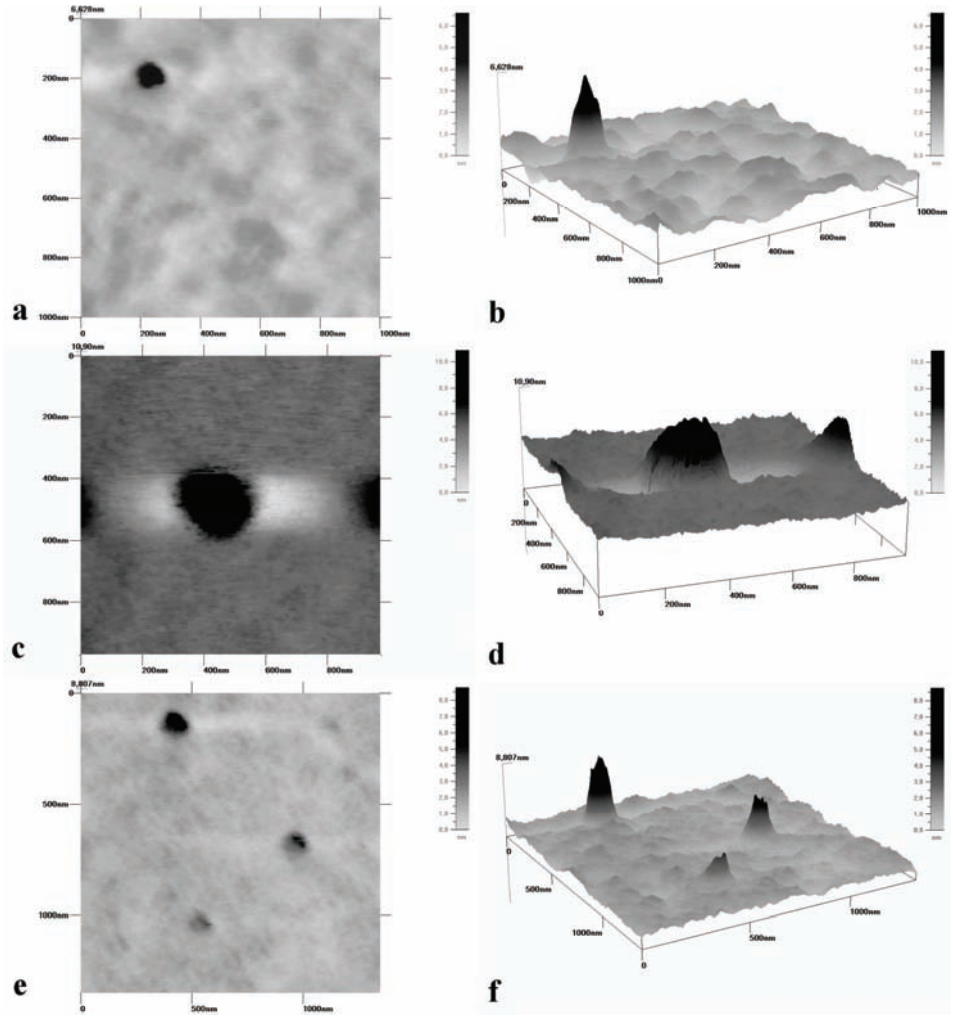

Fig. 1. Top and 3D views of AFM images of C60, C70 and C84 particles, respectively.

Dynamic light scattering (DLS)

Dynamic light scattering measurements were performed to examine the particle size distribution of the three different fullerene-based colloids and the formation of aggregates in the specimens. Based on data presented in Fig. 2, it could be conclude that the sizes of most of the C_{60} particles were between 100–150 nm. The DLS measurements of the C_{70} and C_{84} particles showed that the sizes were approximately the same, between 40–50 nm. Less than 10 % of the C_{70} particles had a diameter in the range from 80 to 100 nm. The mean lateral diameter measured by AFM were larger than the real mean diameters measured by DLS because of convolution of the tip.[20]

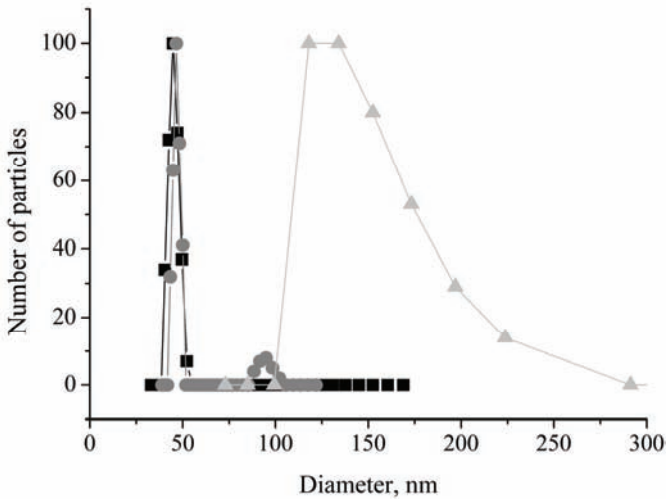

Fig. 2. Particle size distribution of different fullerene particles in the colloids: (●) C_{70} particles, (▲) C_{60} particles, (■)C_{84} particles.

The results obtained by AFM measurements and by DLS for particle size distribution were in a good agreement.

Electron paramagnetic resonance (EPR)

Electron paramagnetic resonance (EPR) is a non-optical technique in which energy transfer between the intrinsic magnetism of an unpaired electron and an external magnetic field is measured with a sensitive microwave detection system. An EPR spectrum is recorded by measuring the strength of the microwave signal when the magnetic field is swept over a small range.[23]

The reaction of $^1\Delta_g$ with a stable molecule can generate a moderately long--lived free radical. In addition, $^1\Delta_g$ can react with a spin label, an organic molecule with an unpaired electron. Determination of the structure of the adduct by EPR provides an unambiguous identification. The spin label TEMP was employed as a spin label probe. The reaction of $^1\Delta_g$ with TEMP leads to the free radical TEMPO.[18]

The results of EPR measurements of the three different fullerene-based colloids are presented in Fig. 3. In a previous study, it was established that singlet oxygen was generated by $n$$C_{60}$.[19] These experimental results were confirmed by a theoretical model.[16] In this study, generation of singlet oxygen by $n$$C_{84}$ was observed. The amplitude of EPR signal produced by $n$$C_{84}$ is significantly higher than the ones caused by $n$$C_{60}$ and $n$$C_{70}$. This is for the first time that the generation of singlet oxygen by C_{84} particles in an aqueous solution is shown. The observed formation rates of Tempo were about two orders of magnitude faster for $n$$C_{84}$ than for $n$$C_{60}$ and $n$$C_{70}$.

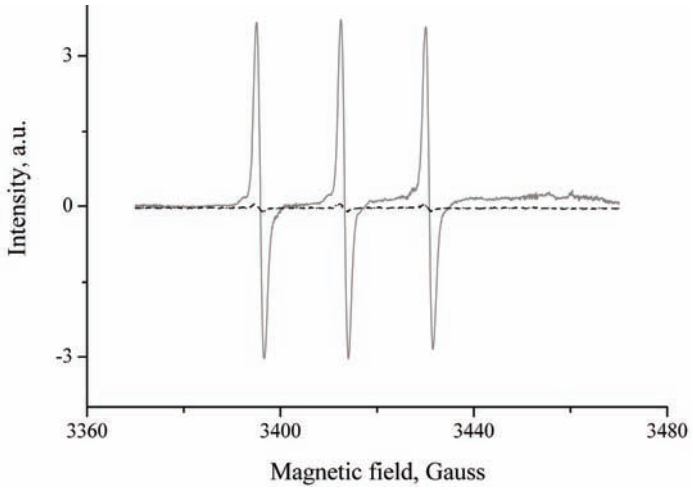

Fig. 3. EPR Spectra of the three different fullerene-based colloids: (···) nC$_{60}$, (-·-·-) nC$_{70}$ and ( ) nC$_{84}$.

Experimentally, seven C_{84} isomers are formed in standard fullerene soot.[24] Of these, the two most abundant isomers are D_2(IV) (*ca*. 50 %) and D_{2d}(II) (*ca*. 25 %). The triplet lifetime of D_2(IV) C_{84} is 640 μs, which represents the second longest time found to date among fullerenes. The triplet lifetimes of C_{60} and C_{70} in toluene at room temperature are 143 μs and 11.8 ms, respectively.[25] The energies of the lowest lying triplet states of C_{60} and C_{70} are 1.62 and 1.54 eV, respectively.[26,27]

Despite the fact that C_{70} has a longer triplet lifetime than C_{60}, the present results demonstrate that nC$_{60}$ and nC$_{70}$ produce almost equal amounts of singlet oxygen. One of the reasons for such behavior is the fact that C_{70} quenches singlet oxygen much better than C_{60}.[28] According to literature data, the rates of singlet oxygen quenching for C_{60} and C_{70} are 6.1×10^4 L mol^{-1} s^{-1} and 3×10^6 L mol^{-1} s^{-1}, respectively.[29,30] Based on a theoretical model of singlet oxygen generation by nC$_{60}$ and nC$_{70}$,[16] the concentration of neutral oxygen inside nC$_{60}$ and nC^{70} is in the range of 10^{14} to 10^{17} cm^{-3}, and nC$_{70}$ produces only 5 % more singlet oxygen than nC$_{60}$.

Booth *et al*. recently showed the presence of a peak at around 0.97 eV in the emission spectrum of C_{84}{D_2(IV)}, which was assigned to luminescence emission to $^1\Delta_g$ molecular oxygen.[31] According to measurement of energies, the lowest lying triplet state of D_2(IV) and D_{2d}(II) are 0.99 and 0.94 eV.[31] No significant emission from $^1\Delta_g$ was observed for D_{2d}(II).[31] Up to now, it was considered that the higher fullerenes produce a significantly lower amount of the reactive form of molecular oxygen $^1O_2(^1\Delta_g)$ than C_{60} and C_{70}.[32]

The extremely high generation of singlet oxygen by nC$_{84}$ compared to nC$_{60}$ and nC$_{70}$ could be, at the moment, explained by two facts. The first one is that the total energy of the triplet state of excited C$_{84}${D$_2$(IV)} is almost identical to the excitation energy of neutral oxygen, 1.6 eV.[31] Therefore, the process of energy transfer from C$_{84}$ to neutral oxygen can proceed without collision with a third body, necessary to take the excess of energy.

The second fact is that the area of the channels in the unit cell of a C$_{84}$ nanocrystal that permits diffusion of neutral oxygen within the unit cell is rather larger than for the unit cell of C$_{60}$ or C$_{70}$. It was reported that a face-centered cubic structure was dominant for C$_{60}$, C$_{70}$ and C$_{84}$.[33–35] Zubov *et al.* assumed free rotation of the nearly spherical fullerene molecules in the unit cells at room temperature.[36]

The distances, a, among the nearest fullerene molecules in a unit cell (C$_{60}$, C$_{70}$ and C$_{84}$) and the surface area of one channel between the fullerene molecules in the unit cell are listed in Table I, from which it can be seen that the distances between the C$_{84}$ molecules are the largest. Since there are six channels per unit cell, the total surface area for the diffusion of neutral oxygen is 9 times larger for C$_{84}$ than for C$_{60}$.

TABLE I. Parameters of fullerene nanocrystals

Property	C$_{60}$	C$_{70}$	C$_{84}$
a / nm	1.417	1.501	1.59
Surface area of one channel ($\times 10^{18}$ m^2)	0.431	0.4835	0.5425

CONCLUSIONS

In this work, the generation of singlet oxygen by a water-based nC$_{84}$ colloid was demonstrated for the first time. The rate of singlet oxygen generation by the nC$_{84}$ colloid was two orders of magnitude higher than those of the nC$_{60}$ and nC$_{70}$ colloid. Experimental conformation was obtained by EPR spectroscopy.

Acknowledgment. This research was supported by the Ministry of Science and Technological Development of the Republic of Serbia (Project No. 145073).

И З В О Д

СТВАРАЊЕ СИНГЛЕТНОГ КИСЕОНИКА У ВОДЕНИМ КОЛОИДИМА ВИШИХ ФУЛЕРЕНА

СВЕТЛАНА П. ЈОВАНОВИЋ[1], ЗОРАН М. МАРКОВИЋ[1], ДУШКА Н. КЛЕУТ[1], ВЛАДИМИР Д. ТРАЈКОВИЋ[2], БРАНКА С. БАБИЋ-СТОЈИЋ[1], МИРОСЛАВ Д. ДРАМИЋАНИН[1] и БИЉАНА М. ТОДОРОВИЋ МАРКОВИЋ[1]

[1]"Винча" Институт за нуклеарне науке, п.пр. 522, 11001 Београд и [2]Институт за микробиологију и имунологију, Медицински факултет, Универзитет у Београду, Др. Суботића 1, 11000 Београд

У овом раду су приказани резултати анализе синтетисаних фулеренских колоида. Фулерени C$_{60}$, C$_{70}$ и C$_{84}$ су коришћени за синтезу водених колоидних раствора. Електронском парамагнетном резонантном спектроскопијом (EPR) селективно је праћено стварање синглетног кисеоника и утврђено је да највећа количина синглетног кисеника настаје у колоиду

nC$_{84}$. EPR сигнал колоида nC$_{84}$ има двоструко већу амплитуду у односу на амплитуде EPR сигнала колоида nC$_{60}$ и nC$_{70}$. Испитана је структура, облик и величина честица добијених колоида микроскопом атомских сила (AFM). На основу AFM анализа утврдили смо да је просечна величина честица 200, 80 и 70 nm за фулеренске колоиде nC$_{60}$, nC$_{70}$ и nC$_{84}$ редом. DLS мерењима такође су испитане величине честица и потврђени резултати добијени AFM испитивањем.

(Примљено 17. јуна 2009, ревидирано 26. априла 2010)

REFERENCES

1. S. Bosi, T. Da Ros, G. Spalluto, M. Prato, *J. Med. Chem.* **38** (2003) 913
2. S. C. Tsang, Y. K. Chen, P. J. F. Harris, M. L. H. Green, *Nature* **372** (1994) 159
3. J. S. Shil, Y. C. Chao, M. F. Sung, G. J. Sau, C. S. Chiou, *Sensors Actuators B* **76** (2001) 347
4. Q. H. Wang, A. A. Setlur, J. M. Lauerhaas, J. Y. Dai, E. W. Scelig, R. P. H. Chang, *Appl. Phys. Lett.* **72** (1998) 2912
5. P. Innocenti, G. Brusatin, *Chem. Mater.* **13** (2001) 3126
6. G. V. Andrievsky, V. K. Klochkov, E. I. Karyankina, N. O. Medlov-Petrossyan, *Chem. Phys. Lett.* **300** (1999) 392
7. J. W. Arbogast, C. S. Foote, *J. Am. Chem. Soc.* **113** (1991) 8886
8. M. Belousova, N. G. Mironova, M. S. Yurev, *Opt. Spectrosc.* **98** (2005) 349
9. T. J. Dougherty, C. J. Gomer, B. W. Henderson, G. Jori, D. Kessel, M. Korbelik, J. Moan, Q. Peng, *J. Natl. Cancer Inst.* **90** (1998) 889
10. Y. Tabata, Y. Murakami, Y. Ikada, *Jpn. J. Cancer Res.* **88** (1997) 1108
11. J. Liu, S. Ohta, A. Sonoda, M. Yamada, M. Yamamoto, N. Nitta, K. Murata, Y. Tabata, *J. Control. Release* **117** (2007) 104
12. J. D. Fortner, D. Y. Lyon, C. M. Sayes, A. M. Boyd, J. C. Falkner, E. M. Hotze, L. B. Alemany, Y. J. Tao, W. Guo, K. D. Ausman, V. L. Colvin, J. B. Hughes, *Environ. Sci. Technol.* **39** (2005) 4307
13. G. V. Andrievsky, M. V. Kosevich, O. M. Vovk, V. S. Shelkovsky, L. A. Vaschchenko, *Chem. Commun.* (1995) 1281
14. S. Deguchi, G. A. Rossitza, K. Tsujii, *Langmuir* **17** (2001) 6013
15. J. Brant, J. Labille, J. Y. Bottero, M. R. Wiener, *Langmuir* **22** (2006) 3878
16. Z. Marković, B. Todorović Marković, D. Kleut, N. Nikolić, S. Vranješ Djurić, M. Misirkić, L. Vučićević, K. Janjetović, A. Isaković, L. Harhaji, B. Babić Stojić, M. Dramićanin, V. Trajković, *Biomaterials* **28** (2007) 5437
17. F. Diederich, R. L. Whetten, *Acc. Chem. Res.* **25** (1992) 119
18. B. Vileno, M. Lekka, A. Sienkiewicz, P. Marcoux, A. J. Kulik, S. Kasas, S. Catsicas, A. Graczyk, L. Forro, *J. Phys. Condens. Matter.* **17** (2005) S1471
19. A. Isaković, Z. Marković, B. Todorović-Marković, N. Nikolić, S. Vranješ-Djurić, M. Mirković, M. Dramićanin, L. Harhaji, N. Raičević, Z. Nikolić, V. Trajković, *Tox. Sci.* **91** (2006) 173
20. M. Rasa, B. W. M. Kuipers, A. P. Philipse, *J. Colloid Interface Sci.* **250** (2002) 303
21. A. Rao, M. Schoenenberger, E. Gnecco, T. Glatzel, E. Meyer, D. Brandlin, L. Scandela, *J. Phys: Conf. Ser.* **61** (2007) 971
22. J. Brant, H. Lecoanet, M. Wiesner, *J. Nanopart. Res.* **7** (2005) 545

23. I. Kruk, *Environmental Toxicology and Chemistry Oxygen Species*, Springer, Berlin, 1998, p. 26
24. T. J. S. Dennis, T. Kai, K. Asato, T. Tomiyama, H. Shinohara, T. Yoshida, Y. Kobayashi, H. Ishiwatari, Y. Miyake, K. Kikuchi, Y. Achiba, *J. Phys. Chem.* **103** (1999) 8747
25. K. D. Ausman, R. B. Weisman, *Res. Chem. Intermed.* **23** (1997) 431
26. J. W. Arbogast, A. P. Darmanyan, C. S. Foote, Y. Rubin, F. N. Diederich, M. M. Alvarez, S. J. Anz, R. L. Whetten, *J. Phys. Chem.* **95** (1991) 11
27. S. P. Sibley, S. M. Argentine, A. H. Francis, *Chem. Phys. Lett*. **188** (1992) 187
28. V. Bagrov, I. M. Belousova, O. B. Danilov, V. M. Kiselev, T. D. Murave'va, E. S. Sasnov, *Opt. Spectrosc*. **102** (2007) 52
29. G. Black, E. Dunkle, E. A. Dorko, L. A. Schlie, *J. Photochem. Photobiol. A* **70** (1993) 147
30. A. Krasnovky, C. S. Foote, *J. Am. Chem. Soc*. **115** (1993) 6013
31. E. C. Booth, S. M. Bachilo, M. Kanai, T. John, S. Dennis, R. B. Weisman, *J. Phys. Chem. C* **111** (2007) 17720
32. L. Juha, B. Ehrenberg, S. Couris, E. Koudoumas, S. Leach, V. Hamplová, Z. A. Müllerová, P. Kubát, *Chem. Phys. Lett*. **335** (2001) 539
33. N. Yao, C. F. Klein, S. K. Behal, M. M. Disko, R. D. Sherwood, D. M. Cox, *Phys. Rev. B* **45** (1992) 11366
34. Y. Saito, Y. Ishikawa, A. Ohshita, H. Shinohara, H. Nagashima, *Phys. Rev. B* **46** (1992) 1846
35. Y. Saito, T. Yoshikawa, N. Fujimoto, H. Shinohara, *Phys. Rev. B* **489** (1993) 9182
36. V. I. Zubov, N. P. Tretiakov, I. V. Zubov, *Eur. Phys. J. B* **17** (2000) 629.